Learning Adaptive Multi-Stage Energy-based Prior for Hierarchical Generative Model

Anonymous authors
Paper under double-blind review

Abstract

Hierarchical generative models represent data with multiple layers of latent variables organized in a top-down structure. These models typically assume Gaussian priors for multi-layer latent variables, which lack expressivity for the contextual dependencies among latents, resulting in a distribution gap between the prior and the learned posterior. Recent works have explored hierarchical energy-based prior models (EBMs) as a more expressive alternative to bridge this gap. However, most approaches learn only a *single* EBM, which can be ineffective when the target distribution is highly multi-modal and multi-scale across hierarchical layers of latent variables. In this work, we propose a framework that learns *multi-stage* hierarchical EBM priors, where a sequence of adaptive stages progressively refines the prior to match the posterior. Our method supports both joint training with the generator and a more efficient two-phase strategy for deeper hierarchies. Experiments across standard benchmarks show that our approach consistently generates higher-quality images and learns richer hierarchical representations.

1 Introduction

Hierarchical generative models, also known as multi-layer generator models, represent data using multiple layers of latent variables arranged in a top-down structure. Top layers typically capture high-level semantics, while bottom layers capture low-level fine details. Such models have shown strong performance in modelling complex data distributions and learning multi-level representations (Child, 2020; Vahdat & Kautz, 2020; Havtorn et al., 2021; Maaløe et al., 2019). The prior distributions over these latent variables are usually assumed to be Gaussian, which mainly capture inter-layer relationships (i.e., dependencies between layers) and ignore intra-layer contextual relationships (i.e., dependencies among latent units within the same layer). This lack of expressivity often leads to a mismatch between the assumed prior and the aggregated posterior learned from data, ultimately degrading the quality of generated samples and the capability of learning hierarchical representations.

Recent advances have introduced energy-based models (EBMs) as more expressive priors (Cui et al., 2023a;b; Aneja et al., 2021). EBMs can model rich intra-layer dependencies, offering a stronger inductive bias and modelling capacity than Gaussians. However, most existing approaches consider only a single EBM ("single-stage") for the complex posterior. When the posterior distribution is highly multi-modal and latent scales differently across layers, learning a single EBM prior is difficult and often ineffective. One line of research seeks to overcome this by borrowing ideas from diffusion models (Cui & Han, 2024; Yu et al., 2022; 2023), which introduce a sequence of conditional EBMs learned at different noise levels. While effective, these approaches depend on carefully designed diffusion schedules and require costly sampling procedures. Another line of work (Xiao & Han, 2022; Rhodes et al., 2020) proposes multi-stage learning for marginal EBMs (Xiao & Han, 2022), which develops a self-adaptive strategy that evolves multiple EBMs without relying on a fixed schedule. Yet, these methods are restricted to *flat* latent spaces, limiting their ability to model hierarchical structures and capture layered representations. As a result, the development of multi-stage hierarchical EBM priors remains largely unexplored.

In this work, we develop multi-stage learning for hierarchical EBM priors. Our framework constructs a sequence of hierarchical EBM priors, viewed as density-ratio estimators, where each stage adaptively refines the prior by treating the previous stage as the new base distribution. This formulation constructs a chain of ratio bridges that progressively align the prior with the posterior, yielding a more robust and tractable solution than single-step methods. Unlike diffusion-based approaches, our method does not require a pre-defined schedule, but instead allows both the generator and hierarchical EBMs to evolve self-adaptively. Compared to flat latent space Adaptive-CE, the multi-scale nature of hierarchical latent space makes sampling across different layers difficult. To address this, we adopt a uni-scale latent space reparameterization (Section 3.2), which transforms the multi-scale latent variables into a consistent space where EBMs can be learned and sampled more effectively. Our framework supports two training schemes: (i) *joint learning*, where the generator and EBMs are optimized together, and (ii) a more efficient *two-phase* strategy for deeper hierarchies, where the generator is trained first and the EBMs are learned afterward as complementary priors.

Extensive experiments across benchmark datasets show that our multi-stage hierarchical EBM prior not only improves image quality but also learns semantically meaningful, layered representations. Ablation studies further validate the benefits of multi-stage learning, uni-scale reparameterization, and the two-phase training strategy. Together, these results demonstrate that multi-stage hierarchical EBMs provide a powerful and scalable alternative to Gaussian or single-step EBM priors in hierarchical generative modelling.

In summary, our main contributions are as follows:

- We propose a novel framework that introduces multi-stage EBM priors for hierarchical generative models, enabling more expressive latent modelling than Gaussian or single-stage EBM prior.
- We adopt a uni-scale latent space reparameterization and develop two training schemes, which improve the effectiveness and efficiency of EBM learning and sampling.
- We perform extensive experiments on standard benchmarks, demonstrating that our approach consistently generates higher-quality samples and learns richer hierarchical representations.

2 Preliminary

2.1 Hierarchical Generative Model

Hierarchical generative models extend the standard latent variable generative model by introducing multiple layers of latent variables arranged in a top-down structure. Each layer captures information at a different level of abstraction, with higher layers encoding global semantics and lower layers modelling fine details. Formally, let $\mathbf{X} \in \mathbb{R}^D$ denote an observed data example in a high-dimensional space, and let $\mathbf{z} \in \mathbb{R}^d$ denote latent variables with $d \ll D$. A hierarchical model defines a joint distribution over $\mathbf{X}$ and a hierarchy of latent variables $\mathbf{Z} = \{\mathbf{z}_1, \ldots, \mathbf{z}_L\}$ through the following factorization:

$$\begin{aligned} p_\beta(\mathbf{X}, \mathbf{Z}) =& p_{\beta_0}(\mathbf{X}|\mathbf{Z}) p_{\beta_{>0}} p(\mathbf{Z}) \quad \text{where} \\ p_{\beta_{>0}}(\mathbf{Z}) =& \prod_{i=1}^{L-1} p_{\beta_i}(\mathbf{z}_i|\mathbf{z}_{i+1}) p_0(\mathbf{z}_L) \end{aligned} \tag{1}$$

$p_{\beta_0}(\mathbf{X}|\mathbf{Z})$ is the generation model parameterized by β_0, while $p_{\beta_{>0}}(\mathbf{Z})$ specifies the hierarchical prior over latent variables. Each conditional dependency $p_{\beta_i}(\mathbf{z}_i|\mathbf{z}_{i+1})$ is modeled as a Gaussian distribution $\mathcal{N}(\mathbf{z}_i; \mu_{\beta_i}(\mathbf{z}_{i+1}), \sigma^2_{\beta_i}(\mathbf{z}_{i+1}))$, where μ_{β_i} and $\sigma^2_{\beta_i}$ denote the mean and diagonal covariance determined by $\mathbf{z}_{i+1}$. At the top of the hierarchy, the prior $p_0(\mathbf{z}_L)$ is typically set to a standard Gaussian.

Although hierarchical generative models provide a powerful framework for learning layered representations through multiple latent variables, their effectiveness is constrained by Gaussian priors. Such priors primarily capture dependencies across layers in the top-down hierarchy, but they fail to model the richer relationships among latent variables within the same layer, i.e., latent units at the same layer are distributed conditionally independent. This limited expressiveness leads to a mismatch between the assumed prior and the true

aggregated posterior, commonly referred to as the prior-hole problem, resulting in degraded generation quality and learned representations.

2.2 Hierarchical Energy-based Prior

Energy-based models (EBMs) are well known for their ability to capture complex dependencies, especially within high-dimensional data or latent spaces (Gao et al., 2020; Pang et al., 2020; Du et al., 2020). When applied to hierarchical generative models, EBMs can act as expressive priors that model richer intra-layer interactions among latent variables (see Figure 1). Notably, JointEBM (Cui et al., 2023a) proposes a hierarchical EBM prior over all latent variables as

$$p_{\omega,\beta_{>0}}(\mathbf{Z}) = \frac{1}{\mathcal{Z}_{\omega,\beta_{>0}}} \exp\left[F_\omega(\mathbf{Z})\right] p_{\beta_{>0}}(\mathbf{Z}) \tag{2}$$

where the energy function $F_\omega(\mathbf{Z}) = \sum_{i=1}^{L} f_\omega(\mathbf{z}_i)$ couples the latent variables across all layers, $p_{\beta_{>0}}(\mathbf{Z})$ is the Gaussian prior defined in Eqn 1, and $\mathcal{Z}_{\omega,\beta_{>0}}$ is the normalizing constant.

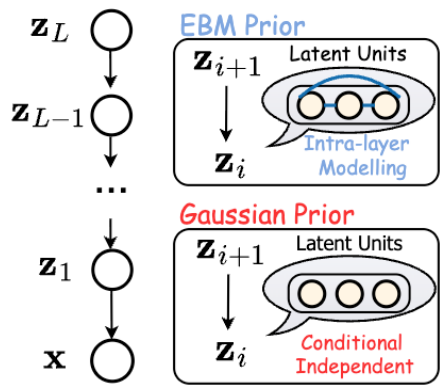

Figure 1: Multi-layer latent variables and latent units.

In contrast, NCP-VAE (Aneja et al., 2021) learns a conditional EBM prior for each intermediate layer, where each conditional EBM prior is defined as

$$\begin{aligned} p_{\omega,\beta_{>0}}(\mathbf{Z}) &= \prod_{i=1}^{L-1} p_{\omega_i,\beta_i}(\mathbf{z}_i|\mathbf{z}_{i+1}) p_{\omega_L}(\mathbf{z}_L) \quad \text{where} \\ p_{\omega_i,\beta_i}(\mathbf{z}_i|\mathbf{z}_{i+1}) &= \frac{1}{\mathcal{Z}_{\omega_i,\beta_i}(\mathbf{z}_{i+1})} \exp[f_{\omega_i}(\mathbf{z}_i)] p_{\beta_i}(\mathbf{z}_i|\mathbf{z}_{i+1}) \end{aligned} \tag{3}$$

The energy function $f_{\omega_i}(\mathbf{z}_i)$ adjusts the Gaussian prior $p_{\beta_i}(\mathbf{z}_i|\mathbf{z}_{i+1})$ with a learnable reweighting.

In both JointEBM and NCP-VAE, the learning objective can be viewed as minimizing the KL divergence between the aggregated posterior $q(\mathbf{Z})$ and the EBM prior $p_{\omega,\beta_{>0}}(\mathbf{Z})$:

$$D_{\mathrm{KL}}(q(\mathbf{Z})||p_{\omega,\beta_{>0}}(\mathbf{Z})) \quad \text{where} \quad q(\mathbf{Z}) = \int p_\beta(\mathbf{Z}|\mathbf{X}) p_{\mathrm{data}}(\mathbf{X}) d\mathbf{X} \tag{4}$$

Although these hierarchical EBM priors demonstrate the capability of modelling intra-layer contextual relationships, providing greater expressivity and capacity than Gaussian priors, learning remains challenging. Specifically, both approaches rely on a single-stage EBM prior to bridge the gap between the aggregated posterior $q(\mathbf{Z})$ and the base Gaussian prior $p_{\beta_{>0}}(\mathbf{Z})$. However, because $q(\mathbf{Z})$ is typically highly multi-modal, forcing a single EBM to approximate the entire distribution is difficult and often leads to suboptimal results.

3 Methodology

3.1 Multi-Stage Density Ratio Estimation

Single-Stage Density Ratio Estimation. Given a target distribution $q(\mathbf{Z})$ and a base distribution $p(\mathbf{Z})$, the goal is to estimate their density ratio $r_\omega(\mathbf{Z}) = q(\mathbf{Z})/p(\mathbf{Z})$[1]. A binary classifier $D_\omega(\mathbf{Z}) : \mathbb{R}^d \to (0,1)$ can be trained to discriminate between samples from $q(\mathbf{Z})$ and $p(\mathbf{Z})$ using the standard binary cross-entropy loss:

$$-\mathbb{E}_{q(\mathbf{Z})}[\log D_\omega(\mathbf{Z})] - \mathbb{E}_{p(\mathbf{Z})}[\log(1 - D_\omega(\mathbf{Z}))] \tag{5}$$

At optimum, $D^*_\omega(\mathbf{Z}) = \frac{q(\mathbf{Z})}{q(\mathbf{Z})+p(\mathbf{Z})}$, yielding the estimator $r_\omega(\mathbf{Z}) = q(\mathbf{Z})/p(\mathbf{Z}) \approx \frac{D^*_\omega(\mathbf{Z})}{1-D^*_\omega(\mathbf{Z})}$.

[1] We assume access to samples from both $q(\mathbf{Z})$ and $p(\mathbf{Z})$.

We can also maximize an equivalent objective $\mathcal{L}(\omega)$ with respect to $r_\omega(\mathbf{Z})$ as

$$\mathbb{E}_{q(\mathbf{Z})}\left[\log \frac{r_\omega(\mathbf{Z})}{1+r_\omega(\mathbf{Z})}\right] + \mathbb{E}_{p_\omega(\mathbf{Z})}\left[\log \frac{1}{1+r_\omega(\mathbf{Z})}\right] \tag{6}$$

This can be viewed as learning an EBM of the form $p_\omega(\mathbf{Z}) = \frac{1}{\mathcal{Z}} r_\omega(\mathbf{Z}) p(\mathbf{Z})$, where $\mathcal{Z}$ is the normalizing constant and $r_\omega(\mathbf{Z})$ is an unconstrained positive function. This procedure is widely known as noise-contrastive estimation (NCE). However, when $q(\mathbf{Z})$ and $p(\mathbf{Z})$ differ substantially, single-stage NCE often fails to provide reliable density ratio estimates (Xiao & Han, 2022).

Multi-Stage Density Ratio Estimation. To overcome the limitations of single-stage estimation, the density ratio can be learned in multiple stages. A sequence of estimators $\{r_{\omega_s}(\mathbf{Z})\}_{s=1}^m$ is constructed, where each stage progressively refines the distribution obtained from the previous one. Formally, the model distribution after m stages is defined as

$$p_{\omega_m}(\mathbf{Z}) = r_{\omega_m}(\mathbf{Z}) \cdot p_{\omega_{m-1}}(\mathbf{Z}) = \prod_{s=1}^{m} r_{\omega_s}(\mathbf{Z}) \cdot p(\mathbf{Z}) \tag{7}$$

which can be viewed as a product of intermediate ratio bridges

$$\frac{q(\mathbf{Z})}{p(\mathbf{Z})} = \frac{q(\mathbf{Z})}{p_{\omega_m}(\mathbf{Z})} \cdot \frac{p_{\omega_m}(\mathbf{Z})}{p_{\omega_{m-1}}(\mathbf{Z})} \cdots \frac{p_{\omega_1}(\mathbf{Z})}{p(\mathbf{Z})} \tag{8}$$

This decomposition allows for smoother and more tractable learning, especially in the presence of highly multi-modal targets. Prior works have explored this idea in different forms: Rhodes et al. (2020) applied a fixed-stage design in data space, but achieved only limited success on simple datasets (e.g., MNIST). Xiao & Han (2022) introduced an adaptive multi-stage scheme in flat latent spaces, but such methods remain limited in their capacity to capture structured, hierarchical representations.

3.2 Toward Hierarchical Energy-based Prior

Directly applying multi-stage NCE to hierarchical latent spaces is non-trivial because of their multi-scale structure and strong inter-layer dependencies. While prior work has studied multi-stage learning in flat spaces (Xiao & Han, 2022), extending it to hierarchical EBMs requires addressing these additional challenges. Inspired by the reparameterization strategy introduced in VAEBM (Xiao et al., 2020), we adopt a uni-scale transformation that maps the original hierarchical latent space $\mathbf{Z}$ into a uni-scale space $\mathbf{W}$. Unlike VAEBM, which applies this idea to single-stage data-space EBM, we leverage the uni-scale space to enable efficient multi-stage learning for hierarchical EBM priors.

Recall that the Gaussian prior $p_{\beta_{>0}}(\mathbf{Z})$ in Eqn 1 is factorized into consecutive conditional Gaussians, $p_{\beta_i}(\mathbf{z}_i|\mathbf{z}_{i+1}) \sim \mathcal{N}(\mu_{\beta_i}(\mathbf{z}_{i+1}), \sigma^2_{\beta_i}(\mathbf{z}_{i+1}))$. Through the standard reparameterization trick, each latent variable can be expressed as $\mathbf{z}_i = \mu_{\beta_i}(\mathbf{z}_{i+1}) + \sigma_{\beta_i}(\mathbf{z}_{i+1}) \cdot \mathbf{w}_i$ where $\mathbf{w}_i \sim \mathcal{N}(0, I_{d_i})$. This defines an invertible mapping $\mathcal{T}_{\beta_{>0}}$ such that $\mathbf{Z} = \mathcal{T}_{\beta_{>0}}(\mathbf{W})$ and $\mathbf{W} = \mathcal{T}^{-1}_{\beta_{>0}}(\mathbf{Z})$. In the $\mathbf{W}$-space, the hierarchical EBM prior can then be expressed as $p_{\omega,\beta_{>0}}(\mathbf{W}) = \frac{1}{\mathcal{Z}_{\omega,\beta_{>0}}} r_\omega(\mathcal{T}_{\beta_{>0}}(\mathbf{W})) p_0(\mathbf{W})$, where $p_0(\mathbf{W})$ is a standard Gaussian with independent components $p_0(\mathbf{w}_i) \sim \mathcal{N}(0, I_{d_i})$.

Building on this representation, we define our multi-stage hierarchical EBM prior as

$$\begin{aligned} \text{On } \mathbf{Z}\text{-Space:} \quad & p_{\omega_m,\beta_{>0}}(\mathbf{Z}) = \prod_{s=1}^{m} r_{\omega_s}(\mathbf{Z}) \cdot p_{\beta_{>0}}(\mathbf{Z}) \\ \text{On } \mathbf{W}\text{-Space:} \quad & p_{\omega_m,\beta_{>0}}(\mathbf{W}) = \prod_{s=1}^{m} r_{\omega_s}(\mathcal{T}_{\beta_{>0}}(\mathbf{W})) \cdot p_0(\mathbf{W}) \end{aligned} \tag{9}$$

On $\mathbf{Z}$-Space, the base distribution is Gaussian prior (Eqn. 1), and the multi-stage modelling aims to approximate the target distribution adaptively and progressively. On $\mathbf{W}$-Space, this formulation leverages the uni-scale reparameterization to make multi-stage learning feasible in hierarchical EBMs. The transformation $\mathcal{T}$ preserves hierarchical dependencies, while the $\mathbf{W}$-space provides a consistent representation that enables efficient training and sampling.

3.3 Learning Multi-Stage Hierarchical Energy-based Prior

3.3.1 Joint Learning

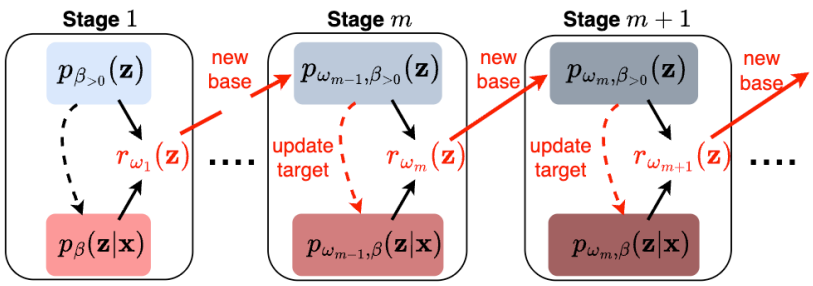

Figure 2: Updating schema of **joint learning**. At each stage m, a density ratio $r_{\omega_m}(\mathbf{Z})$ is estimated by contrastive learning, distinguishing samples from the prior and from the aggregated posterior. Posterior samples are obtained via MCMC posterior sampling with the prior of the current stage (red dashed line), while prior samples can be taken from posterior samples at the previous stage. The estimated ratio is then used to update the prior, which becomes the base distribution for the next stage. By repeating this process, the prior is progressively refined across stages, enabling stable joint learning of both the generator and the hierarchical EBM prior.

With hierarchical EBM prior, we can specify a joint distribution of the hierarchical generative model as

$$p_{\omega_m,\beta}(\mathbf{X},\mathbf{Z}) = p_{\beta_0}(\mathbf{X}|\mathbf{Z})p_{\omega_m,\beta_{>0}}(\mathbf{Z}) \tag{10}$$

which involves generator parameters β and multiple stages of EBM parameters ω. Learning can be achieved by iterating between the maximum likelihood estimation (MLE) of β and contrastive estimation of ω.

Specifically, at the m-th stage, updating the generator parameters β corresponds to maximizing the data likelihood. The gradient takes the form

$$\mathbb{E}_{p_{\text{data}}(\mathbf{X})p_{\omega_m,\beta}(\mathbf{Z}|\mathbf{X})}\left[\frac{\partial}{\partial\beta}\log p_{\beta_0}(\mathbf{X}|\mathbf{Z})\right] + \mathbb{E}_{p_{\text{data}}(\mathbf{X})p_{\omega_m,\beta}(\mathbf{Z}|\mathbf{X})}\left[\frac{\partial}{\partial\beta}\log p_{\beta_{>0}}(\mathbf{Z})\right] \tag{11}$$

where $p_{\omega_m,\beta}(\mathbf{Z}|\mathbf{X})$ denotes the generator posterior. These expectations are approximated by posterior sampling using Markov Chain Monte Carlo (MCMC), such as Langevin dynamics (see Eqn 15).

The EBM parameters ω_m are updated via contrastive estimation, where the generator posterior serves as the target distribution and the prior from the previous stage serves as the base distribution:

$$\mathbb{E}_{p_{\text{data}}(\mathbf{X})p_{\omega_{m-1},\beta}(\mathbf{Z}|\mathbf{X})}\left[\frac{\partial}{\partial\omega_m}\log\frac{r_{\omega_m}(\mathbf{Z})}{1+r_{\omega_m}(\mathbf{Z})}\right] + \mathbb{E}_{p_{\omega_{m-1},\beta}(\mathbf{Z})}\left[\frac{\partial}{\partial\omega_m}\log\frac{1}{1+r_{\omega_m}(\mathbf{Z})}\right] \tag{12}$$

where samples from $p_{\omega_{m-1},\beta}(\mathbf{Z})$ are also obtained using Langevin dynamics.

Since the hierarchical latent variables $\mathbf{Z}$ are inherently multi-scale, both posterior sampling and EBM sampling are carried out in the uni-scale $\mathbf{W}$-space. The results are then mapped back to $\mathbf{Z}$-space through the transformation function $\mathcal{T}$ for gradient computation. This joint learning procedure alternates between updating β and ω at each stage, gradually refining both the generator and the hierarchical EBM prior. More efficiently, once the density ratio estimator achieves sufficient accuracy, the prior samples from $p_{\omega_{m-1},\beta}(\mathbf{Z})$ can be replaced by samples from the posterior $p_{\omega_{m-1},\beta}(\mathbf{Z}|\mathbf{X})$, thereby bypassing MCMC sampling from the prior and reducing computational cost (Xiao & Han, 2022).

While joint learning provides a principled way to train both the generator and the hierarchical EBM prior together, it relies heavily on MCMC posterior sampling. This procedure becomes increasingly inefficient as the hierarchy deepens, since each MCMC step requires backpropagation through all latent layers of the generator.

3.3.2 Two-phase Learning for Deep Hierarchy

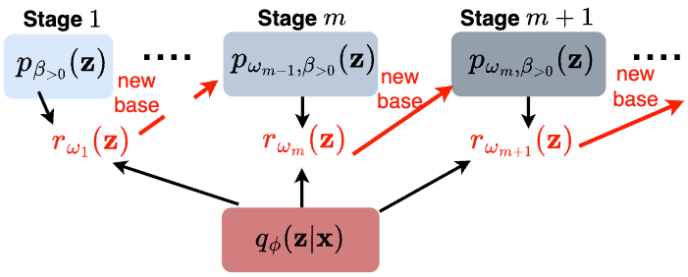

Figure 3: Updating schema of **two-phase** learning. In the second phase, the variational posterior $q_\phi(\mathbf{Z}|\mathbf{X})$ serves as the *fixed* target distribution for hierarchical EBM prior learning. At each stage m, a density ratio $r_{\omega_m}(\mathbf{Z})$ is estimated between $q_\phi(\mathbf{Z}|\mathbf{X})$ and the current base prior. The updated prior $p_{\omega_m,\beta_{>0}}(\mathbf{Z})$ is then used as the base distribution for the next stage.

To address this computational bottleneck, we introduce a two-phase learning strategy. In the first phase, we approximate the generator posterior using a variational inference model, which eliminates the need for costly posterior MCMC. In the second phase, our multi-stage EBM prior is learned on top of this fixed variational posterior, retaining the expressiveness of the EBM while ensuring scalability to deep hierarchical structures.

First-phase: Variational Learning with Gaussian Prior. Variational learning Sø nderby et al. (2016) introduces an inference model $q_\phi(\mathbf{Z}|\mathbf{X})$ that approximates the generator posterior distribution. For hierarchical latent variables, the inference model is also structured hierarchically, i.e., $q_\phi(\mathbf{Z}|\mathbf{X}) = q_{\phi_1}(\mathbf{z}_1|\mathbf{X}) \prod_{i=2}^{L} q_{\phi_i}(\mathbf{z}_i|\mathbf{z}_{i-1})$, where each conditional factor is modeled as a Gaussian distribution.

With such inference model, variational learning proceeds by maximizing the evidence lower bound (ELBO)

$$\mathbb{E}_{p_{\text{data}}(\mathbf{X})q_\phi(\mathbf{Z}|\mathbf{X})}\left[\log \frac{p_\beta(\mathbf{X},\mathbf{Z})}{q_\phi(\mathbf{Z}|\mathbf{X})}\right] = \mathbb{E}_{p_{\text{data}}(\mathbf{X})q_\phi(\mathbf{Z}|\mathbf{X})}\left[\log p_{\beta_0}(\mathbf{X}|\mathbf{Z})\right] - \mathbb{E}_{p_{\text{data}}(\mathbf{X})}[D_{\text{KL}}(q_\phi(\mathbf{Z}|\mathbf{X})||p_{\beta_{>0}}(\mathbf{Z}))] \quad (13)$$

By maximizing the ELBO, we effectively maximize a lower bound of the true log-likelihood. The gap between the ELBO and the likelihood is given by the KL divergence term, ELBO $= \log p_\beta(\mathbf{X}) - D_{\text{KL}}(q_\phi(\mathbf{Z}|\mathbf{X})||p_\beta(\mathbf{Z}|\mathbf{X}))$, which encourages the variational posterior to approximate the generator posterior. In other words, variational learning can be interpreted as approximate MLE, where the inference model provides a tractable surrogate for posterior sampling. Once the inference model is well trained, its variational posterior $q_\phi(\mathbf{Z}|\mathbf{X})$ serves as a reliable approximation of $p_\beta(\mathbf{Z}|\mathbf{X})$, and can therefore be adopted as the target distribution in the second phase of our hierarchical EBM prior learning.

Second-phase: Contrastive Estimation with Fixed Generator. In the second phase, we fix both the generator parameters β and the inference network ϕ, and focus on learning the hierarchical EBM prior. The training objective at stage m is

$$\mathbb{E}_{p_{\text{data}}(\mathbf{X})q_\phi(\mathbf{Z}|\mathbf{X})}\left[\frac{\partial}{\partial \omega_m}\log\frac{r_{\omega_m}(\mathbf{Z})}{1+r_{\omega_m}(\mathbf{Z})}\right] + \mathbb{E}_{p_{\omega_{m-1},\beta}(\mathbf{Z})}\left[\frac{\partial}{\partial \omega_m}\log\frac{1}{1+r_{\omega_m}(\mathbf{Z})}\right] \quad (14)$$

where posterior samples are efficiently obtained from the fixed inference model. Conceptually, this phase isolates the task of refining the prior: it learns to bridge the gap between the aggregated posterior $q_\phi(\mathbf{Z})$ and the base Gaussian prior $p_{\beta_{>0}}(\mathbf{Z})$, without requiring costly posterior MCMC updates.

This two-phase design offers two key advantages. First, it makes training significantly more efficient in deep hierarchical settings by decoupling generator learning from EBM refinement. Second, unlike most existing methods (Aneja et al., 2021; Xiao et al., 2020; Cui et al., 2023a; Dai & Wipf, 2019) that attempt to close this gap with a single-stage EBM, we decompose the process into multiple adaptive stages. Each stage provides refinement of the prior, yielding smoother convergence and a more faithful approximation of complex, multi-modal posteriors.

3.3.3 Markov Chain Monte Carlo Sampling

Both training strategies require access to hierarchical latent variables from either the generator posterior or the EBM prior. To do so, we adopt MCMC sampling, such as Langevin dynamics (Neal et al., 2011), in the uni-scale space. Specifically, for an arbitrary distribution $p(\mathbf{z})$, it is performed as

$$\mathbf{z}_{\tau+1} = \mathbf{z}_\tau + s\frac{\partial}{\partial \mathbf{z}_\tau}\log p(\mathbf{z}_\tau) + \sqrt{2s}U_\tau \tag{15}$$

where τ indexes the time step, s is the step size and U_τ is Gaussian noise.

MCMC for EBM Prior. To sample from the hierarchical EBM prior, we apply Langevin dynamics in the uni-scale $\mathbf{W}$-space. The gradient update combines contributions from all ratio functions r_{ω_s} together with the standard Gaussian reference prior.

$$\text{EBM: } \frac{\partial}{\partial \mathbf{W}_\tau}\left[\sum_{s=1}^{m}\log r_{\omega_s}(\mathcal{T}_{\beta>0}(\mathbf{W}_\tau)) - \frac{||\mathbf{W}_\tau||^2}{2}\right] \quad \text{Posterior: } \frac{\partial}{\partial \mathbf{W}_\tau}\left[\log p_\beta(\mathbf{X}, \mathcal{T}_{\beta>0}(\mathbf{W}_\tau)) - \frac{||\mathbf{W}_\tau||^2}{2}\right] \tag{16}$$

MCMC for Generator Posterior. Similarly, for generator posterior, we also perform Langevin dynamics in uni-scale $\mathbf{W}$-space. MCMC sampling in the uni-scale ensures effective sampling for both prior and posterior distributions, while the transformation $\mathcal{T}$ maps the results back to the original hierarchical latent space.

4 Related Work

Hierarchical Generative Models. Hierarchical generative models employ multiple layers of latent variables organized in a top-down structure and are typically parameterized with Gaussian priors (Vahdat & Kautz, 2020; Child, 2020; Sønderby et al., 2016; Maaløe et al., 2019; Sø nderby et al., 2016). While convenient, Gaussian priors lack statistical expressivity, often leading to the prior-hole problem and degraded generation quality (Aneja et al., 2021; Cui et al., 2023a). To overcome this limitation, recent studies have explored expressive priors such as EBMs, but most approaches rely on single-stage learning. Our work extends this line of research by developing multi-stage hierarchical EBM priors that more effectively capture complex posterior distributions while remaining scalable to deep hierarchies.

Energy-based Models. EBMs have been widely applied in data space for modeling images and other high-dimensional signals (Du et al., 2020; Gao et al., 2020; Han et al., 2020b; Cui & Han, 2023; Hill et al., 2022; Xiao et al., 2020). Extensions to latent space exist in both flat (Pang et al., 2020; Yu et al., 2024) and hierarchical settings (Aneja et al., 2021; Cui et al., 2023a;b), but these methods adopt single-stage estimation, limiting their ability to approximate multi-modal posteriors. Multi-stage training has recently been studied in flat latent spaces (Xiao & Han, 2022), showing that a sequence of density ratio estimators can improve learning stability. However, extending this idea to hierarchical latent spaces introduces new challenges due to scale differences and inter-layer dependencies. Our work addresses these challenges with a uni-scale reparameterization and develops a self-adaptive multi-stage framework for hierarchical EBMs, enabling robust and scalable training across deep latent structures.

Diffusion Energy-based Models. Both diffusion frameworks and multi-stage learning approximate complex distributions by constructing a sequence of intermediate models. Diffusion methods learn conditional EBMs (e.g., $p_\omega(\mathbf{W}_t|\mathbf{W}_{t+1})$) guided by a pre-defined forward noise process (Cui & Han, 2024; Gao et al., 2020). While effective, this conditioning restricts each EBM to local refinements and requires carefully designed schedules. In contrast, our multi-stage framework builds marginal models (e.g., $p_{\omega_m}(\mathbf{W}) = \prod_{s=1}^{m} r_{\omega_s}(\mathbf{W})p_0(\mathbf{W})$) in a self-adaptive manner, allowing each stage to refine the prior distribution without a fixed noise schedule.

From a learning perspective, diffusion-based EBMs are typically trained with MLE, which requires costly inner-loop MCMC sampling at every step. Our approach leverages contrastive estimation, which optimizes density ratios and avoids repeated inner-loop MCMC. During sampling, diffusion models require $K \times T$ MCMC steps across all reverse steps, whereas our method needs only a single round of MCMC over the final multi-stage prior. This results in substantial efficiency gains, while maintaining expressivity and scalability.

5 Experiments

5.1 Latent Space Modeling

Figure 4: Synthesis on CelebA-HQ-256 (left), LSUN-Church-64 (center), and CIFAR10 (right).

We first evaluate our method on the task of latent space modeling. A well-learned hierarchical EBM prior should produce informative latent samples that, when passed through the generator, yield high-quality and realistic synthesis. Concretely, we generate images by sampling $\mathbf{W}$ from the learned EBM prior, mapping it into hierarchical latent variables $\mathbf{Z} = \mathcal{T}_{\beta_{>0}}(\mathbf{W})$, and decoding with the generator $p_{\beta_0}(\mathbf{X}|\mathbf{Z})$. We benchmark across several datasets, including SVHN Netzer et al. (2011), CIFAR-10 Krizhevsky et al. (2009), CelebA-64 Liu et al. (2014), LSUN-Church-64 Yu et al. (2015), and high-resolution CelebA-HQ-256 Karras et al. (2017). Image quality is measured with Fréchet Inception Distance (FID) and Inception Score (IS).

Joint Learning. We evaluate our framework under a joint training scheme with a two-layer ($L = 2$) hierarchical latent structure, where the generator and the multi-stage hierarchical EBM prior are learned jointly. We compare against several groups of baselines. (i) *Flat latent models with multi-stage EBMs*, such as Adaptive-CE Xiao & Han (2022), which learns multi-stage priors but only in single-layer latent spaces. (ii) *Hierarchical models with single-stage EBMs*, including Joint-EBM Cui et al. (2023a) and NCP-VAE Aneja et al. (2021), which extend EBMs to hierarchical structures but rely on a single-stage formulation. (iii) *Other expressive priors and Gaussian-based hierarchical models*, such as LEBM Pang et al. (2020), Diffusion-Amortized Yu et al. (2024), and 2s-VAE Dai & Wipf (2019), as well as LVAE Sønderby et al. (2016), Short-run MCMC (SRI) Nijkamp et al. (2020), and BIVA Maaløe et al. (2019).

As shown in Table 1, our method consistently achieves superior results across datasets. These results suggest that introducing a multi-stage EBM prior into hierarchical latent spaces offers advantages over both single-stage EBMs and flat multi-stage approaches, resulting in stronger priors and improved generation quality.

Table 1: Joint learning for FID (↓) comparison.

Method	SVHN	CelebA-64	CIFAR-10
Ours	**20.42**	**29.12**	**61.12**
Adaptive CE	26.19	35.38	65.01
Joint-EBM	26.81	33.60	66.32
NCP-VAE	33.23	42.07	78.06
LEBM	29.44	37.87	70.15
Diffusion-Amortized	21.17	35.67	60.89
2s-VAE	33.23	42.07	78.06
BIVA	31.65	33.58	66.37
LVAE (L=5)	39.26	53.40	-
SRI (L=5)	35.32	47.95	-

Table 2: Two-phase learning for FID (↓) comparison.

Method	CelebA-HQ-256	LSUN-Church-64
Ours	**7.84**	**6.65**
Hierarchical Diff-EBM Cui & Han (2024)	8.78	7.34
Joint-EBM Cui et al. (2023a)	9.89	8.38
NCP-VAE Aneja et al. (2021)	24.79	-
NVAE* Vahdat & Kautz (2020)	30.25	38.13
NVAE*-Recon	1.64	2.45
DRL-EBM ($T = 6$) Gao et al. (2020)	-	7.04
Adv-EBM Yin et al. (2020)	17.31	10.84
GLOW Kingma & Dhariwal (2018)	68.93	59.35
PGGAN Karras et al. (2017)	8.03	6.42

Table 3: Two-phase learning on CIFAR-10.

Methods	IS (↑)	FID (↓)
Ours	**9.03**	**7.80**
Hierarchical Diff-EBM Cui & Han (2024)	9.03	8.93
Joint-EBM Cui et al. (2023a)	8.99	11.34
NCP-VAE Aneja et al. (2021)	-	24.08
Multi-layer Generator		
NVAE* Vahdat & Kautz (2020)	5.30	37.73
NVAE*-Recon	-	0.68
HVAE Sø nderby et al. (2016)	-	81.44
BIVA Maaløe et al. (2019)	-	66.37
Energy-based Models		
Dual-MCMC Cui & Han (2023)	8.55	9.26
Architectural-EBM Cui et al. (2023b)	-	63.42
DRL-EBM ($T = 6$) Gao et al. (2020)	8.40	9.58
Adaptive-CE Xiao & Han (2022)	-	65.01
VAEBM Xiao et al. (2020)	8.43	12.19
Hat EBM Hill et al. (2022)	-	19.15
ImprovedCD Du et al. (2020)	7.85	25.1
Divergence Triangle Han et al. (2020a)	-	30.10
Adv-EBM Yin et al. (2020)	9.10	13.21
GANs+Score+Diffusion Models		
StyleGANv2 w/o ADA Karras et al. (2020)	8.99	9.9
Diffusion-Amortized Yu et al. (2024)	-	57.72
NCSN Song & Ermon (2019)	8.87	25.32
LSGM Vahdat et al. (2021)	-	2.10
DDPM ($T = 1000$) Ho et al. (2020)	9.46	3.17

Two-Phase Learning. For deep hierarchical structures, our multi-stage hierarchical EBM prior is learned as ratio bridges between the fixed aggregate posterior and the base Gaussian prior. Once learned, this EBM prior serves as a more informative alternative to the Gaussian prior, enabling generation of realistic samples.

Following the setup of prior works, including Hierarchical Diff-EBM Cui & Han (2024), Joint-EBM Cui et al. (2023a), and NCP-VAE Aneja et al. (2021), we build on top of NVAE Vahdat & Kautz (2020) as our backbone model (denoted NVAE*). As shown in Table 2 and Table 3, our method achieves competitive or superior performance, even when compared to recent diffusion-based approaches. Notably, it yields substantial improvements over the NVAE* baseline, highlighting the efficacy of our multi-stage learning strategy in capturing complex latent distributions.

5.2 Analysis of Hierarchical Representation

A hallmark of hierarchical generative models is that different latent layers capture different levels of abstraction: bottom-layer variables tend to encode low-level visual attributes, while top-layer variables capture high-level semantic concepts. In this section, we demonstrate the capability of our multi-stage hierarchical EBM prior in learning hierarchical representations.

5.2.1 Hierarchical Controllable Synthesis

Figure 5: Starting from random samples, attributes such as gender, eyeglasses, and hair color can be manipulated in a top-down order. Higher-layer latents govern semantic structure (e.g., gender, identity), while lower-layer latents refine local appearance (e.g., eyeglasses, hair). Importantly, sampling at lower layers preserves the semantics imposed by higher layers, enabling interpretable and fine-grained controllability across the hierarchy.

A unique advantage of our framework is that controllability emerges naturally from the multi-stage EBM prior, even when the backbone generator is trained in a fully unsupervised manner. Inspired by (Salimans et al., 2016), which demonstrated how GAN discriminators can be repurposed for classification, we reinterpret each stage of our multi-stage NCE framework as a learned discriminator.

Given K class labels or attributes (denoted by y), the hierarchical EBM prior can be extended into a multi-class classifier with $K+1$ outputs, where the $(K+1)$-th logit continues to distinguish posterior samples from prior samples. This formulation enables modeling of the joint distribution $p_{\omega_m,\beta_{m,\geq 0}}(\mathbf{W}, y)$, allowing conditional generation under a specified label y.

As illustrated in Figure 5, our method leverages the discriminative structure of the multi-stage EBM prior to achieve fine-grained and semantically consistent controllability. The hierarchical organization further ensures that semantic structure imposed by higher layers is preserved when lower layers are sampled, enabling controllable generation that is both structured and coherent across different levels of abstraction.

5.2.2 Hierarchical Out-of-Distribution Detection.

Beyond generation and representation learning, our multi-stage hierarchical EBM prior also provides a natural mechanism for out-of-distribution (OOD) detection. Each stage of the prior operates as a density-ratio classifier, distinguishing samples from the aggregated posterior versus the base prior in latent space. As a result, OOD detection emerges as a built-in capability of our framework, requiring no additional supervision or auxiliary objectives.

We evaluate this property by training on CIFAR-10 as the in-distribution dataset and testing on SVHN as OOD. Detection is based on the classifier output $D : \mathbb{R}^d \to (0, 1)$, where lower values indicate higher likelihood of being OOD. As shown in Figure 6, AUROC scores increase with depth: top-layer latents provide the strongest OOD signals by encoding distribution-specific semantics, while lower layers capture more generic features that are often shared across datasets Havtorn et al. (2021).

AUROC	$L^{>0}$	$L^{>3}$	$L^{>6}$	$L^{>9}$	$L^{>12}$
Stage 1	0.3312	0.3858	0.4118	0.4312	0.4410
Stage 2	0.3501	0.3953	0.4315	0.4626	0.5235
Stage 3	0.4045	0.4775	0.4969	0.5351	0.5713
AUROC	$L^{>15}$	$L^{>18}$	$L^{>21}$	$L^{>24}$	$L^{>27}$
Stage 1	0.5382	0.6683	0.6735	0.6960	0.7079
Stage 2	0.6416	0.7277	0.7335	0.7471	0.8002
Stage 3	0.6652	0.7835	0.7710	0.8469	0.8897

Table 4: AUROC (↑) for OOD detection. $L > k$ denotes for using the top k layers. The total number of layers is 30.

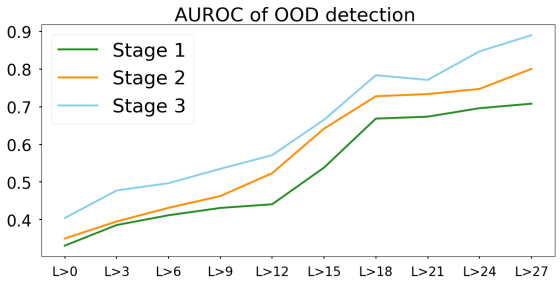

Figure 6: Visualization of AUROC curve.

These findings highlight a key advantage of our hierarchical design. By aligning representation depth with semantic specificity, our model not only improves generative modeling but also enhances robustness to distributional shifts. In particular, the top layers act as semantic sentinels that sharply delineate in-distribution from OOD inputs, making hierarchical EBMs a powerful tool for reliable and interpretable uncertainty estimation.

5.3 Analysis of Multi-Stage Learning Dynamic

5.3.1 Multi-Stage Learning Analysis

We next analyze the learning behavior of our multi-stage framework. In our formulation, each stage of density ratio estimation refines the prior by building on the ratio estimator learned in the previous stage, effectively evolving the base distribution toward the target posterior. As the base distribution becomes progressively better aligned with the posterior, the discrimination task between posterior and prior samples naturally becomes harder. This increasing difficulty is reflected in higher loss values observed in later stages.

Figure 7 illustrates this trend: the average loss (aggregated across all latent layers) grows as the stage index increases. This progression confirms that successive stages refine increasingly aligned priors, making the classification task progressively more challenging. In other words, earlier stages correct large mismatches between the prior and posterior, while later stages focus on finer adjustments. Such behavior is consistent with theoretical expectations and aligns with prior observations in flat latent settings Xiao & Han (2022). These results provide strong empirical support for the effectiveness and robustness of our multi-stage learning scheme.

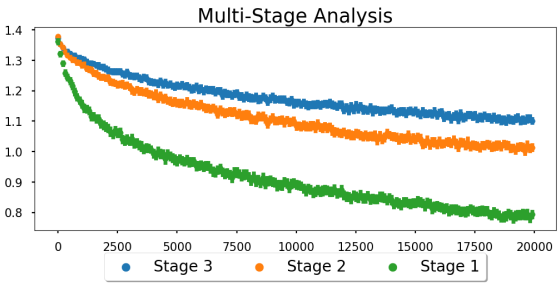

Figure 7: Visualization of stage-wise evolution with loss trends averaged across all latent layers.

5.3.2 Multi-Layer Learning Analysis

To further examine learning dynamics, we analyze loss trends across different latent layers. In hierarchical latent structures, lower layers typically encode fine-grained, low-level details such as texture or background. These features are often more variable and complex, creating a larger gap between the aggregate posterior and the base prior. Consequently, the density ratio estimation task at lower layers is relatively easier, yielding lower loss values.

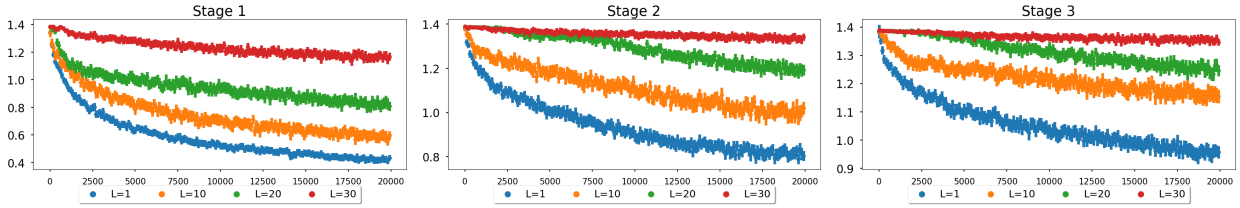

Figure 8: Visualization of layer-wise evolution from stage 1 to stage 3.

This trend is evident in Figure 8, where lower layers consistently report smaller losses than top layers. As additional learning stages are introduced, the multi-stage EBM prior progressively narrows the gap between the posterior and the base distribution at each layer. This refinement makes the classification task more difficult across all layers, leading to higher losses over time. The observed progression confirms that our multi-stage framework effectively reduces discrepancies at every level of the hierarchy, supporting stable and coherent prior learning in complex multi-layer latent spaces.

5.4 Analysis of Energy Landscape

5.4.1 Joint Langevin Transition.

We analyze the sampling behavior using Langevin transition. Starting from a sample drawn from the standard Gaussian, we perform 10 Langevin steps for learned multi-stage hierarchical EBM priors. As illustrated in Figure 9, image quality improves gradually and coherently with each step. This smooth evolution reflects the well-structured energy landscape of our model, which is further facilitated by operating in the uni-scale $\mathbf{u}$-space.

Figure 9: Joint Langevin transition.

5.4.2 Progressive Transition

Figure 10: Visualization of progressive Langevin transition.

We next examine whether each stage of the EBM prior can serve as a base distribution for the subsequent stage. To this end, we perform progressive sampling: at the s-th stage, Langevin dynamics is applied only with the s-th stage EBM prior, initialized from the final sample of the $s-1$ stage. Figure 10 shows that each stage produces a refined update of the sample, demonstrating that the sequence of EBMs provides a coherent progression that incrementally shapes the energy landscape.

5.5 Ablation Studies

Multi-Stage vs. Single-Stage under Fixed Iterations. We begin by testing the effectiveness of the proposed multi-stage framework. To ensure fairness, we fix the total training budget to 15K iterations and compare two settings: (i) a *single-stage* hierarchical EBM prior trained for the full 15K iterations, and (ii) a *three-stage* model, where 5K iterations are allocated to each stage.

As reported in Table 5, the multi-stage approach substantially outperforms the single-stage baseline, achieving an FID of 9.48 compared to 15.15. Notably, the table also reveals a clear progression: Stage 1 starts weaker due to limited training, but each subsequent stage produces marked improvements, with the final stage delivering the strongest results.

This experiment highlights our framework: rather than relying on prolonged training of a single-stage EBM prior, decomposing the task into multiple adaptive stages provides a more effective refinement process. Even with the same computational budget, multi-stage learning achieves higher-quality EBM priors and better generative performance, suggesting that the learning scheme itself is crucial to success.

Table 5: Comparison of single-stage vs. multi-stage learning under a fixed total of 15K training iterations.

Iteration	Single-stage (15K)	Stage 1 (5K)	Stage 2 (5K)	Stage 3 (5K)
FID	15.15	18.68	12.87	9.48

Effect of Langevin step. Each stage in our framework employs Langevin dynamics to draw samples from the EBM prior refined by the previous stage. Our default setting uses $K = 10$ Langevin steps, but we also examine the effect of varying K. As shown in Table 6, performance improves as K increases: reducing to $K = 5$ yields weaker results (FID = 11.15), while increasing to $K = 15$ produces a substantial gain (FID = 7.11). This trend confirms that more accurate sampling enhances prior quality and improves generative performance. Nevertheless, since larger K values also increase computational overhead, we adopt $K = 10$ as a balanced default across experiments.

Table 6: Impact of Langevin steps K and number of stages M on generation quality for CelebA-HQ-256.

CIFAR-10	$K = 5$	$K = 15$	$K = 10$, $M = 3$	$M = 4$
FID	11.15	7.11	**7.84**	7.05

Effect of Stage Number. We also analyze the influence of the number of stages M in the multi-stage learning framework. With $M = 3$, the model achieves strong generative quality (FID = 7.84). Increasing the number of stages to $M = 4$ further reduces the FID to 7.05, indicating that additional stages continue to refine the prior and improve performance. However, the performance gain is relatively modest compared to the increase in training cost and computational complexity. This observation suggests that while deeper staging can yield incremental improvements, three stages provide an effective balance between accuracy and efficiency. Consequently, we adopt $M = 3$ as the default setting for all reported experiments.

Impact of Network Structure and Decoder Type. In our default configuration, the NVAE backbone employs a discretized logistic decoder. To further evaluate the robustness of our approach, we also experiment with the NVAE backbone using a Gaussian decoder and network structures, consistent with the setting in NCP-VAE Aneja et al. (2021). As shown in Table 7, our multi-stage learning consistently outperforms the single-stage baseline, achieving substantially lower FID scores. These results demonstrate that the benefits of our multi-stage framework are not tied to a specific decoder choice, but generalize across network structures.

Table 7: Effect of decoder type on CIFAR-10.

CIFAR-10	Gaussian prior	Stage 1	Stage 2
NCP-VAE	52.45	24.08	-
Ours	52.45	20.68	14.04

6 Conclusion

We proposed a novel framework for learning hierarchical energy-based priors through a multi-stage learning scheme. Instead of relying on a single-stage EBM to approximate the highly complex aggregated posterior, our method progressively refines the prior via a sequence of ratio estimators in a uni-scale latent space. This design enables efficient sampling, stable training, and scalable integration with hierarchical generators.

Comprehensive experiments across multiple benchmarks show that our approach not only improves image generation quality but also yields semantically structured and interpretable latent representations. Moreover, we demonstrated its unique strengths in hierarchical controllability, out-of-distribution detection, and energy landscape analysis

References

Jyoti Aneja, Alex Schwing, Jan Kautz, and Arash Vahdat. A contrastive learning approach for training variational autoencoder priors. *Advances in neural information processing systems*, 34:480–493, 2021.

Rewon Child. Very deep vaes generalize autoregressive models and can outperform them on images. *arXiv preprint arXiv:2011.10650*, 2020.

Jiali Cui and Tian Han. Learning energy-based model via dual-mcmc teaching. *arXiv preprint arXiv:2312.02469*, 2023.

Jiali Cui and Tian Han. Learning latent space hierarchical ebm diffusion models. *arXiv preprint arXiv:2405.13910*, 2024.

Jiali Cui, Ying Nian Wu, and Tian Han. Learning joint latent space ebm prior model for multi-layer generator. In *Proceedings of the IEEE/CVF Conference on Computer Vision and Pattern Recognition (CVPR)*, pp. 3603–3612, June 2023a.

Jiali Cui, Ying Nian Wu, and Tian Han. Learning hierarchical features with joint latent space energy-based prior. In *Proceedings of the IEEE/CVF International Conference on Computer Vision (ICCV)*, pp. 2218–2227, October 2023b.

Bin Dai and David Wipf. Diagnosing and enhancing vae models. *arXiv preprint arXiv:1903.05789*, 2019.

Yilun Du, Shuang Li, Joshua Tenenbaum, and Igor Mordatch. Improved contrastive divergence training of energy based models. *arXiv preprint arXiv:2012.01316*, 2020.

Ruiqi Gao, Yang Song, Ben Poole, Ying Nian Wu, and Diederik P Kingma. Learning energy-based models by diffusion recovery likelihood. *arXiv preprint arXiv:2012.08125*, 2020.

Tian Han, Erik Nijkamp, Linqi Zhou, Bo Pang, Song-Chun Zhu, and Ying Nian Wu. Joint training of variational auto-encoder and latent energy-based model. In *Proceedings of the IEEE/CVF Conference on Computer Vision and Pattern Recognition (CVPR)*, June 2020a.

Tian Han, Erik Nijkamp, Linqi Zhou, Bo Pang, Song-Chun Zhu, and Ying Nian Wu. Joint training of variational auto-encoder and latent energy-based model. In *Proceedings of the IEEE/CVF Conference on Computer Vision and Pattern Recognition*, pp. 7978–7987, 2020b.

Jakob D Drachmann Havtorn, Jes Frellsen, Soren Hauberg, and Lars Maaløe. Hierarchical vaes know what they don't know. In *International Conference on Machine Learning*, pp. 4117–4128. PMLR, 2021.

Mitch Hill, Erik Nijkamp, Jonathan Mitchell, Bo Pang, and Song-Chun Zhu. Learning probabilistic models from generator latent spaces with hat ebm. *Advances in Neural Information Processing Systems*, 35: 928–940, 2022.

Jonathan Ho, Ajay Jain, and Pieter Abbeel. Denoising diffusion probabilistic models. *Advances in Neural Information Processing Systems*, 33:6840–6851, 2020.

Tero Karras, Timo Aila, Samuli Laine, and Jaakko Lehtinen. Progressive growing of gans for improved quality, stability, and variation. *arXiv preprint arXiv:1710.10196*, 2017.

Tero Karras, Miika Aittala, Janne Hellsten, Samuli Laine, Jaakko Lehtinen, and Timo Aila. Training generative adversarial networks with limited data. *Advances in Neural Information Processing Systems*, 33:12104–12114, 2020.

Durk P Kingma and Prafulla Dhariwal. Glow: Generative flow with invertible 1x1 convolutions. *Advances in neural information processing systems*, 31, 2018.

Alex Krizhevsky, Geoffrey Hinton, et al. Learning multiple layers of features from tiny images. 2009.

Ziwei Liu, Ping Luo, Xiaogang Wang, and Xiaoou Tang. Deep learning face attributes in the wild. *CoRR*, abs/1411.7766, 2014. URL `http://arxiv.org/abs/1411.7766`.

Lars Maaløe, Marco Fraccaro, Valentin Liévin, and Ole Winther. Biva: A very deep hierarchy of latent variables for generative modeling. *Advances in neural information processing systems*, 32, 2019.

Radford M Neal et al. Mcmc using hamiltonian dynamics. *Handbook of markov chain monte carlo*, 2(11):2, 2011.

Yuval Netzer, Tao Wang, Adam Coates, Alessandro Bissacco, Bo Wu, and Andrew Y. Ng. Reading digits in natural images with unsupervised feature learning. In *NIPS Workshop on Deep Learning and Unsupervised Feature Learning 2011*, 2011. URL `http://ufldl.stanford.edu/housenumbers/nips2011_housenumbers.pdf`.

Erik Nijkamp, Bo Pang, Tian Han, Linqi Zhou, Song-Chun Zhu, and Ying Nian Wu. Learning multi-layer latent variable model via variational optimization of short run mcmc for approximate inference. In *European Conference on Computer Vision*, pp. 361–378. Springer, 2020.

Bo Pang, Tian Han, Erik Nijkamp, Song-Chun Zhu, and Ying Nian Wu. Learning latent space energy-based prior model. *Advances in Neural Information Processing Systems*, 33:21994–22008, 2020.

Benjamin Rhodes, Kai Xu, and Michael U Gutmann. Telescoping density-ratio estimation. *Advances in neural information processing systems*, 33:4905–4916, 2020.

Tim Salimans, Ian Goodfellow, Wojciech Zaremba, Vicki Cheung, Alec Radford, and Xi Chen. Improved techniques for training gans. *Advances in neural information processing systems*, 29, 2016.

Casper Kaae Sø nderby, Tapani Raiko, Lars Maalø e, Søren Kaae Sø nderby, and Ole Winther. Ladder variational autoencoders. In D. Lee, M. Sugiyama, U. Luxburg, I. Guyon, and R. Garnett (eds.), *Advances in Neural Information Processing Systems*, volume 29. Curran Associates, Inc., 2016. URL `https://proceedings.neurips.cc/paper/2016/file/6ae07dcb33ec3b7c814df797cbda0f87-Paper.pdf`.

Casper Kaae Sønderby, Tapani Raiko, Lars Maaløe, Søren Kaae Sønderby, and Ole Winther. Ladder variational autoencoders. *Advances in neural information processing systems*, 29, 2016.

Yang Song and Stefano Ermon. Generative modeling by estimating gradients of the data distribution. *Advances in Neural Information Processing Systems*, 32, 2019.

Arash Vahdat and Jan Kautz. Nvae: A deep hierarchical variational autoencoder. *Advances in Neural Information Processing Systems*, 33:19667–19679, 2020.

Arash Vahdat, Karsten Kreis, and Jan Kautz. Score-based generative modeling in latent space. *Advances in Neural Information Processing Systems*, 34:11287–11302, 2021.

Zhisheng Xiao and Tian Han. Adaptive multi-stage density ratio estimation for learning latent space energy-based model. *arXiv preprint arXiv:2209.08739*, 2022.

Zhisheng Xiao, Karsten Kreis, Jan Kautz, and Arash Vahdat. Vaebm: A symbiosis between variational autoencoders and energy-based models. *arXiv preprint arXiv:2010.00654*, 2020.

Xuwang Yin, Shiying Li, and Gustavo K Rohde. Analyzing and improving generative adversarial training for generative modeling and out-of-distribution detection. *arXiv preprint arXiv:2012.06568*, 2020.

Fisher Yu, Yinda Zhang, Shuran Song, Ari Seff, and Jianxiong Xiao. Lsun: Construction of a large-scale image dataset using deep learning with humans in the loop. *arXiv preprint arXiv:1506.03365*, 2015.

P Yu, S Xie, X Ma, B Jia, B Pang, R Gao, Y Zhu, S-C Zhu, and YN Wu. Latent diffusion energy-based model for interpretable text modeling. In *International Conference on Machine Learning (ICML 2022)*., 2022.

Peiyu Yu, Yaxuan Zhu, Sirui Xie, Xiaojian Ma, Ruiqi Gao, Song-Chun Zhu, and Ying Nian Wu. Learning energy-based prior model with diffusion-amortized mcmc. *arXiv preprint arXiv:2310.03218*, 2023.

Peiyu Yu, Yaxuan Zhu, Sirui Xie, Xiaojian Shawn Ma, Ruiqi Gao, Song-Chun Zhu, and Ying Nian Wu. Learning energy-based prior model with diffusion-amortized mcmc. *Advances in Neural Information Processing Systems*, 36, 2024.

A Additional Result

Joint v.s. progressive sampling.

We compare the two strategies quantitatively. As shown in Table 8, progressive sampling can yield slightly better generation quality, but at a much higher computational cost, since each stage requires separate Langevin updates. Joint sampling, in contrast, delivers strong performance with far greater efficiency, making it the default strategy in our framework. This analysis confirms that our multi-stage hierarchical EBM prior supports both flexible stage-wise refinement and efficient joint sampling.

Table 8: FID for image synthesis of different stages.

	Prgrogressive Sampling			Joint Sampling
	Stage 1	Stage 2	Stage 3	
CIFAR-10	13.15	9.72	7.62	7.80
LSUN-Church-64	14.82	10.06	6.12	6.65
CelebA-HQ-256	11.48	8.65	7.71	7.84

Stage-wise Analysis with Diffusion Scheme. Both diffusion-based EBMs and our multi-stage contrastive framework progressively refine the prior distribution by decomposing the modeling task into simpler intermediate steps. Tabble 9 compares the generation quality (FID) of intermediate stages.

While both approaches improve with more refinement stages, our method shows clear advantages. Diffusion-based models rely on fixed schedules and Gaussian perturbations, which restrict flexibility and may lead to inefficient sampling. In contrast, our multi-stage framework is self-adaptive, where each stage learns the density ratio between its evolving prior and the target posterior, which ultimately yields better generative quality.

Table 9: Comparison of diffusion-based and multi-stage priors across refinement steps. $t = (2, 1, 0)$ denotes diffusion steps; $s = (1, 2, 3)$ denotes stages in our multi-stage hierarchical EBM prior.

FID	Gaussian Prior	$t = 2$ / $s = 1$	$t = 1$ / $s = 2$	$t = 0$ / $s = 3$
CIFAR-10	37.73	18.11 / 13.15	11.87 / 9.72	8.93 / 7.62
LSUN-Church-64	38.13	20.15 / 14.82	13.54 / 10.06	7.31 / 6.12
CelebA-HQ-256	30.25	17.75 / 11.48	12.05 / 8.65	8.78 / 7.71

We show additional image synthesis in Figure 11, Figure 12, and Figure 13, as well as Langevin transition results in Figure 14.

B Derivation

For conditional Gaussian distribution $p_{\beta_i}(\mathbf{z}_i|\mathbf{z}_{i+1})$, we define an invertible transformation function $T_{\beta_{>0}}$. Take 2-layer latent variables as an example,

$$\begin{aligned} \mathbf{z}_2 &= T^{\mathbf{z}_2}_{\beta_{>0}}(\mathbf{u}_2) = \mathbf{u}_2 \ \text{ and} \\ \mathbf{z}_1 &= T^{\mathbf{z}_1}_{\beta_{>0}}(\mathbf{u}_1, \mathbf{u}_2) = \mu_{\beta_1}(\mathbf{z}_2) + \sigma_{\beta_1}(\mathbf{z}_2) \cdot \mathbf{u}_1 \end{aligned} \tag{17}$$

where $\mathbf{u}_1$ and $\mathbf{u}_2$ are distributed as independent Gaussian noise, i.e., $(\mathbf{u}_1, \mathbf{u}_2) \sim p_0(\mathbf{u}_1, \mathbf{u}_2)$ and $p_0(\mathbf{u}_1, \mathbf{u}_2) = p_0(\mathbf{u}_1)p_0(\mathbf{u}_2)$ with each $p_0(\mathbf{u}_i) \sim \mathcal{N}(0, I_d)$. By the change-of-variable rule, we have

$$\begin{aligned} p_{\beta_{>0}}(\mathbf{z}_1, \mathbf{z}_2) &= p_0(\mathbf{u}_1, \mathbf{u}_2)|\det(J_{T^{-1}_{\beta_{>0}}})| \ \text{ and} \\ p_0(\mathbf{u}_1, \mathbf{u}_2) &= p_{\beta_{>0}}(\mathbf{z}_1, \mathbf{z}_2)|\det(J_{T_{\beta_{>0}}})| \end{aligned} \tag{18}$$

where $J_{T_{\beta>0}}$ is the Jacobian of $T_{\beta>0}$.

For joint EBM prior on $\tilde{\mathbf{z}}$-space $p_{\omega,\beta>0}(\tilde{\mathbf{z}}) = \frac{1}{\mathrm{Z}} r_\omega(\tilde{\mathbf{z}})) p_{\beta>0}(\tilde{\mathbf{z}})$, we can apply the change-of-variable rule and Eqn. 18 as

$$\begin{aligned} p_{\omega,\beta>0}(\tilde{\mathbf{u}}) &= p_{\omega,\beta>0}(\tilde{\mathbf{z}}) |\det(J_{T_{\beta>0}})| \\ &= \frac{1}{\mathrm{Z}} r_\omega(T_{\beta>0}(\tilde{\mathbf{u}})) p_{\beta>0}(\tilde{\mathbf{z}}) |\det(J_{T_{\beta>0}})| \\ &= \frac{1}{\mathrm{Z}} r_\omega(T_{\beta>0}(\tilde{\mathbf{u}})) p_0(\tilde{\mathbf{u}}) \end{aligned} \tag{19}$$

With such single-stage EBM prior on $\tilde{\mathbf{u}}$-space, we construct our multi-stage EBM prior.

C Implementation Detail

Training detail. For joint learning, we benchmark our method on CIFAR-10, SVHN, and CelebA-64, for which we scale training images to $[-1, 1]$ and use only 40,000 examples of CelebA-64 following Xiao & Han (2022). For Two-phase training, we train our model on CIFAR-10, LSUN-Church-64, and CelebA-HQ-256 using the same setting as NVAE Vahdat & Kautz (2020). We compute FID scores using 30,000 generated images for CelebA-HQ-256 and 50,000 for other datasets.

We use one A100 Nvidia GPU (training time on CIFAR-10 for 0.15 seconds/iteration) for joint learning and two A100 Nvidia GPUs (training time on CIFAR-10 for 8.45 seconds/iteration) for Two-phase training.

Network Structure. For joint learning, we adopt the network structures from Xiao & Han (2022), which contain generator and energy function networks shown in Table 11. For Two-phase learning scheme, we utilize the NVAE[2] backbone model, and our energy function is shown in Table 10.

Figure 11: Additional synthesis on LSUN-Church-64.

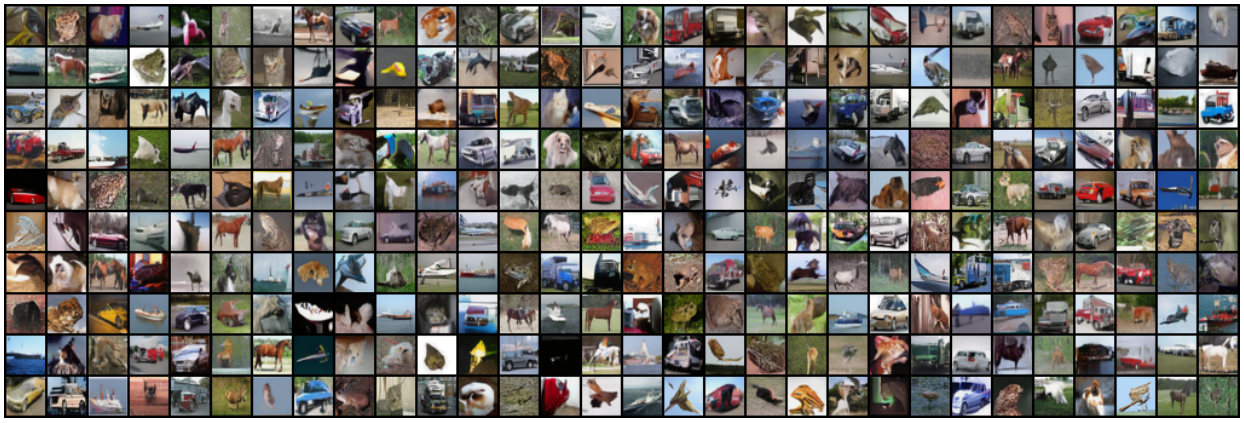

Figure 12: Additional synthesis on CIFAR-10.

[2]https://github.com/NVlabs/NVAE

Figure 13: Additional synthesis on CelebA-HQ-256 with temp= 1.0 (left) and temp= 0.7 (right).

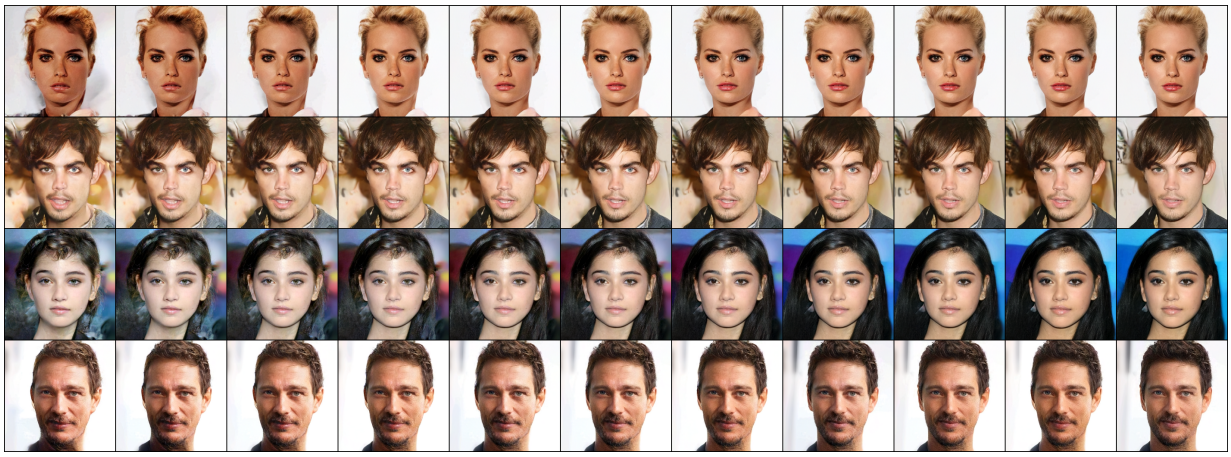

Figure 14: Additional Langevin transition on LSUN-Church-64, CIFAR-10, and CelebA-HQ-256.

Figure 15: Additional progressive Langevin transition on LSUN-Church-64, CIFAR-10, and CelebA-HQ-256.

Table 10: Two-phase learning energy function on each $\mathbf{z}_i$.

Conv Residule Block (in-ch, out-ch, downsample, preActivation)	
Input: SiLU(h_0) if preActivation else h_0	
$h_1(h_0)$ = 4x4 conv (out-ch), s=2, SiLU	if downsample
$h_1(h_0)$ = 3x3 conv (out-ch), s=1, SiLU	if not downsample
$h_1(h_1)$ = 3x3 conv (out-ch)	if in-ch$\neq$out-ch or downsample
$h_{\text{short}}(h_0)$ = 4x4 conv (out-ch), s=2	if downsample
$h_{\text{short}}(h_0)$ = 3x3 conv (out-ch), s=1	if in-ch$\neq$out-ch
$h_{\text{short}}(h_0) = h_0$	else
return $h_1 + h_{\text{short}}$	
Conv Residule (in-ch, out-ch, res-layer)	
Input: h_0	
Conv Residule Block (in-ch, out-ch, downsample=True, preActivation=True)	
#res-layer x Conv Residule Block (in-ch, out-ch, downsample=False, preActivation=True)	
Linear Residule Block (in-ch, out-ch, preActivation)	
Input: SiLU(h_0) if preActivation else h_0	
$h_1(h_0)$ = Linear (out-ch), SiLU	-
$h_1(h_1)$ = Linear (out-ch)	if in-ch$\neq$out-ch
$h_{\text{short}}(h_0)$ = Linear (out-ch)	if in-ch$\neq$out-ch
$h_{\text{short}}(h_0)$=h_0	else
return $h_1 + h_{\text{short}}$	
Energy function (nef=128, ndf=256, res-layer=8)	
Layer	In-Out Size
Input: $\mathbf{u}_i$	h x w x ch
3x3 conv (nef), s=1	h x w x nef
# of Conv Residule (nef, nef, res-layer)	4 x 4 x 64
flatten	$4 * 4 * 64$
# res-layer of Linear Residule Block (ndf, ndf, preActivation=True)	ndf
SiLU, Linear (1)	1

Table 11: 2-layer generator network on CIFAR-10.

$p_{\beta_0}(\mathbf{x}\|\mathbf{z}_1)$, ngf= 64		
Layers	In-Out Size	Stride
Input: $\mathbf{z}_1$	1 x 1 x 100	-
4x4 convT (ngf x 8), LReLU	4 x 4 x (ngf x 8)	1
4x4 convT (ngf x 4), LReLU	8 x 8 x (ngf x 4)	2
4x4 convT (ngf x 2), LReLU	16 x 16 x (ngf x 2)	2
4x4 convT (3), Tanh	32 x 32 x 3	2
$p_{\beta_1}(\mathbf{z}_1\|\mathbf{z}_2)$, ngf= 256		
Layers	In-Out Size	
Input: $\mathbf{z}_2$	100	
Linear (ngf), LReLU	ngf	
Linear (ngf), LReLU	ngf	
Linear (ngf), LReLU	ngf	
Linear (ngf), LReLU	ngf	
Linear (100), μ of $\mathbf{u}_1$	100	
Linear (100), $\log\sigma$ of $\mathbf{u}_1$	100	
energy function for each $\mathbf{u}_i$, ndf= 200		
Layers	In-Out Size	
Input: $\mathbf{z}_1$	100	
Linear (ngf), LReLU	ndf	
Linear (ngf), LReLU	ndf	
Linear (ngf), LReLU	ndf	
Linear (ngf), LReLU	ndf	
Linear (1)	1	